


Photoinduced Phase Transitions in Ferroelectrics

Charles Paillard,^{1,2,*} Engin Torun,³ Ludger Wirtz,³ Jorge Íñiguez,^{4,3} and Laurent Bellaïche^{1,†}¹*Department of Physics and Institute for Nanoscience and Engineering, University of Arkansas, Fayetteville, Arkansas 72701, USA*²*Laboratoire Structures, Propriétés et Modélisation des Solides, CentraleSupélec, UMR CNRS 8580, Université Paris-Saclay, 91190 Gif-sur-Yvette, France*³*Physics and Materials Science Research Unit, University of Luxembourg, 162a avenue de la Faiencerie, L-1511 Luxembourg, Luxembourg*⁴*Materials Research and Technology Department, Luxembourg Institute of Science and Technology (LIST), Avenue des Hauts-Fourneaux 5, L-4362 Esch/Alzette, Luxembourg*
 (Received 2 December 2018; revised manuscript received 10 April 2019; published 21 August 2019)

Ferroc materials naturally exhibit a rich number of functionalities, which often arise from thermally, chemically, or mechanically induced symmetry breakings or phase transitions. Based on density functional calculations, we demonstrate here that light can drive phase transitions as well in ferroelectric materials such as the perovskite oxides lead titanate and barium titanate. Phonon analysis and total energy calculations reveal that the polarization tends to vanish under illumination, to favor the emergence of nonpolar phases, potentially antiferroelectric, and exhibiting a tilt of the oxygen octahedra. Strategies to tailor photoinduced phases based on phonon instabilities in the electronic ground state are also discussed.

DOI: 10.1103/PhysRevLett.123.087601

Ferroelectric materials possess a spontaneous electric polarization that is switchable by electric fields. Active research in bandgap engineering [1] and unconventional photovoltaic mechanisms [2–4] have prompted perovskite oxide ferroelectrics as potential light absorbers to convert light into electric [5], mechanical [6–8], or chemical energy [9], or for optical memory writing [10] and nondestructive reading [11]. Numerous works focused on the photoinduced deformation of the unit cell without apparent symmetry breaking [8]. However, a recent experimental work hinted at possible structural phase transitions occurring in ferroelectric BaTiO₃ nanowires under illumination [12]. Using first-principles calculations, we show that photoinduced phase transitions are indeed possible in ferroelectrics such as barium and lead titanates. In both cases, transitions to nonpolar phases are predicted. Furthermore, material engineering strategies based on competing lattice instabilities are suggested to tailor the critical concentration of photoinduced carriers at which the transition occurs, thus opening the way to a rational design of materials exhibiting specific properties under illumination.

ABO₃ perovskite oxides are versatile materials exhibiting a wide range of properties (magnetism, polar distortions, etc.). Their high symmetry reference structure (see Fig. 1) is cubic with the *B* cation enclosed in an octahedral cage of oxygens at the center and the *A* cation at the edges of the cube. Simple atomic displacement patterns—e.g., octahedra tilts or electric dipoles sketched in Fig. 1—make it possible to obtain various symmetry breakings and control the materials properties. For convenience, here we denote the most

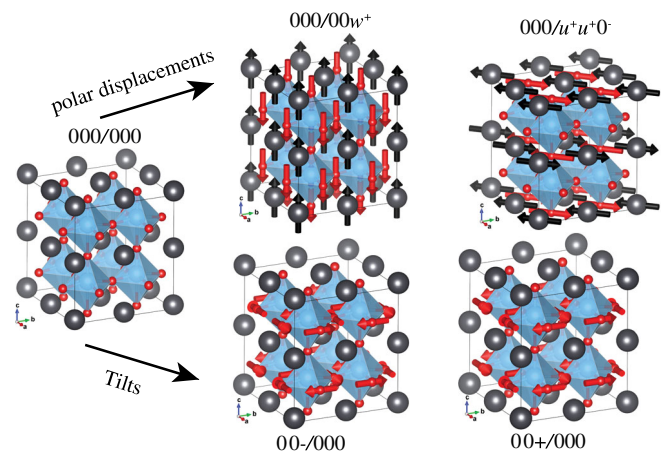


FIG. 1. Sketch of a $2 \times 2 \times 2$ supercell in the paraelectric cubic reference structure $000/000$. A and B cations are in black and blue, oxygens in red. The symmetry of a phase is denoted by (i) its oxygen octahedra tilt pattern $\alpha\beta\gamma$, where α , β , and γ are either 0 (no tilt), “+” (in-phase tilt), or “-” (antiphase tilt) and represent whether the oxygen octahedra tilts around the first, second, and third pseudocubic axes, respectively. Similarly, we denote the electric dipole pattern using a Glazer-like notation $u^{\alpha}v^{\beta}w^{\gamma}$, in which u , v , w represent the magnitude of the dipole inside the perovskite five-atom cell, and α , β , and γ describe whether dipole vectors $[uvw]$ are aligned parallel (“+”) or antiparallel (“-”) when moving by one perovskite five-atom cell along the first, second, and third pseudocubic direction. Typical polar ($000/00w^{+}$), antipolar ($000/u^{+}u^{+}0^{-}$), in-phase ($00c^{+}/000$), and antiphase tilt ($00c^{-}/000$) displacement patterns are depicted using arrows.

relevant of such distortions using a generalized and simplified Glazer notation [13] $\alpha\beta\gamma/u^\alpha v^\beta w^\gamma$, which is introduced in the caption of Fig. 1.

Among perovskite oxides, barium titanate (BTO) and lead titanate (PTO) are prototypical ferroelectric materials. They exhibit a number of phases [14,15] associated with lattice instabilities of the reference cubic phase [16]. The transitions between phases are commonly driven by temperature [14,15], pressure [17–19], or static electric fields [20]. Here, we demonstrate that light can also act as a knob to control the crystal symmetry. Optical manipulation of ferroic materials has mainly focused on the transient manipulation of the ferroic order parameter, relying on nonthermalized photoexcited carriers [21] or strong anharmonic phonon couplings [22]. In contrast, we presently describe the emergence of new phases caused by modified lattice instabilities in the presence of thermalized photo-excited carriers, i.e., the electrons lying at the bottom of the conduction band (CB) and the equal number of holes sitting at the top of the valence band (VB) of a semiconductor during illumination. To this end, we used *ab initio* calculations, detailed in the next section, before examining the cases of barium and lead titanate, respectively. Finally, we discuss the origin of this phenomenon and test design strategies for the engineering of photo-induced phase transitions in ferroelectrics.

We performed density functional theory (DFT) calculations using the Abinit package software [23], with the projector augmented wave method [24,25]. We employ a $2 \times 2 \times 2$ supercell (with respect to the five-atom pseudocubic perovskite cell) containing 40 atoms. The k -point mesh used was a Γ -centered $8 \times 8 \times 8$ grid; the plane-wave cutoff was 35 hartrees. A Fermi-Dirac distribution with

0.1 eV smearing was used to populate the electronic states. The electronic density was considered converged when the difference in the calculated forces between two self-consistent field (SCF) steps was smaller than 10^{-8} hartree bohr $^{-1}$. The structural relaxation was stopped when all the forces on the atoms were smaller than 5×10^{-7} hartree bohr $^{-1}$ and all components of the stress tensor smaller than 0.1 MPa. BTO was described using the PBESol [26] exchange-correlation functional, while the local density approximation [27,28] was employed to treat PTO. Photo-excited thermalized carriers are mimicked using Fermi-Dirac distribution with two quasi-Fermi-levels μ_e and μ_h , as commonly used to describe photovoltaic effects in, for instance, p - n junctions [29]. As a result, during our DFT calculations, the density is self-consistently converged under the constraint of having $n_e = n_{\text{ph}}$ (and $n_h = n_{\text{ph}}$) electrons (holes) in the CB (VB). In other words, at each SCF iteration, the following system of equations

$$n_h = \sum_{i \leq N_v} \sum_{k, \sigma} w_k [1 - f(\varepsilon_{ik, \sigma}, \mu_h)], \quad (1)$$

$$n_e = \sum_{i > N_v} \sum_{k, \sigma} w_k f(\varepsilon_{ik, \sigma}, \mu_e), \quad (2)$$

is solved for μ_e and μ_h using a bisection algorithm. In the above equation, w_k is the weight of k -point \mathbf{k} , $f(\varepsilon_{ik}, \mu)$ is the occupation number (Fermi-Dirac distribution) of state with eigenvalue ε_{ik} ; σ denotes the spin. N_v is the index of the highest valence band. We assume that there is no closing of the gap during our constrained DFT calculations, which is in practice observed for the concentrations of photo-excited carrier pairs n_{ph} considered in this work.

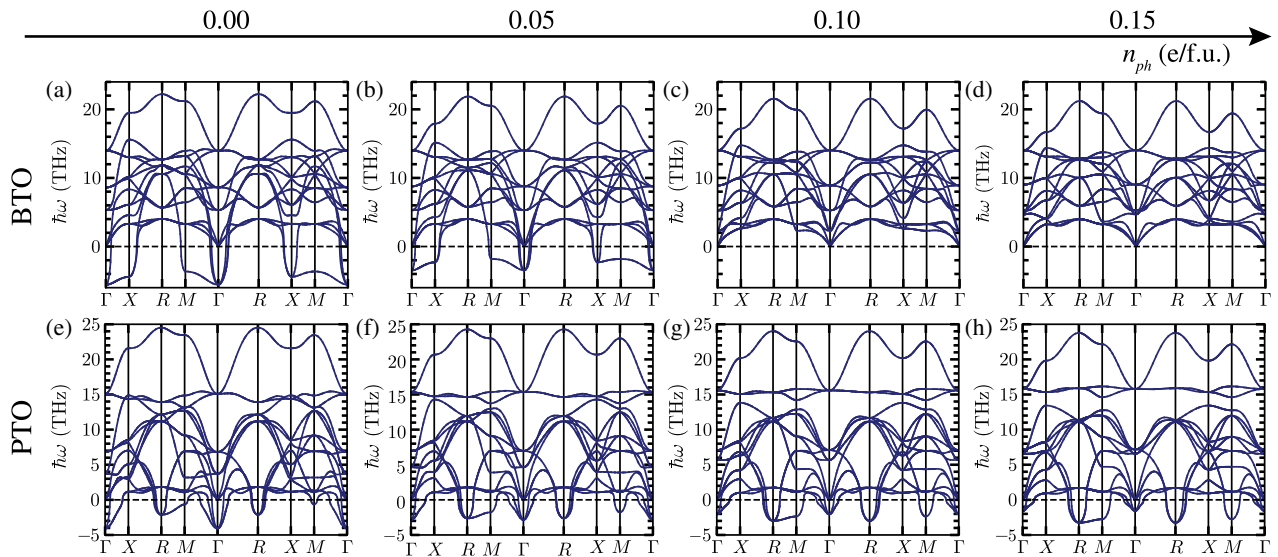


FIG. 2. (a)–(d) Phonon band structure in paraelectric cubic BTO and (e)–(h) PTO for different concentrations of photoexcited carrier pairs $n_{\text{ph}} = 0.00$ e/f.u. (a),(e); $n_{\text{ph}} = 0.05$ e/f.u. (b),(f); $n_{\text{ph}} = 0.10$ e/f.u. (c),(g); and $n_{\text{ph}} = 0.15$ e/f.u. (d),(h). The polar Γ dominant instability in BTO becomes stabilized (i.e., positive and real frequency) for $n_{\text{ph}} \geq 0.10$ e/f.u., as shown in (c) and (d). In PTO, the polar instability at Γ is replaced by a nonpolar tilted instability at M and R .

Note that all structures considered in this work were geometrically relaxed under the photo-excitation constraint mentioned above. The criteria for convergence of the structural degrees of freedom are set to be the same as in electronic ground state calculations.

Phonon calculations using the Phonopy package [30] were performed in the dark and under excitation on the cubic perovskite oxides using a $2 \times 2 \times 2$ supercell after the system was structurally relaxed. No analytic correction, and thus no LO-TO splitting was considered, as the required Born effective charges cannot be calculated in photo-excited cases.

We first calculated the phonon band structure of cubic BTO in Figs. 2(a)–2(d) for different concentrations of photoexcited carriers n_{ph} . In the dark [$n_{ph} = 0$ electron per formula unit (e/f.u.), Fig. 2(a)], the phonon dispersion exhibits imaginary (negative in the figure) frequency modes characteristic of lattice instabilities. The main instability, at Γ , is responsible for the emergence of the polar order in BTO [16], which goes from a high temperature cubic 000/000 structure to a ferroelectric tetragonal 000/00 w^+ phase below ~ 393 K, then to an orthorhombic structure 000/0 v^+v^+ below ~ 280 –270 K and finally to a rhombohedral 000/ $u^+u^+u^+$ phase below ~ 183 K [14]. Upon increasing the number of photo-excited carrier pairs to $n_{ph} = 0.05$ e/f.u. [in Fig. 2(b)], the frequencies of unstable modes along the X - M - Γ path get closer to real (positive) values, the ferroelectric soft optical mode at Γ becoming less unstable. Furthermore, for $n_{ph} \geq 0.1$ e/f.u. [Figs. 2(c) and 2(d)], the cubic phase no longer exhibits unstable phonon modes and is *dynamically stable*!

We calculated the energy [see Fig. 3(a)] of the four phases naturally occurring in bulk BTO, 000/000 (green squares), 000/00 w^+ (blue diamonds), 000/0 v^+v^+ (violet triangles), and 000/ $u^+u^+u^+$ (ground state at 0 K in dark conditions, black dashed baseline). The rhombohedral phase has the lowest energy for low concentrations of photo-excited carriers (up to ≈ 0.0375 e/f.u.), while the tetragonal phase is slightly more stable at intermediate concentrations ($n_{ph} \approx 0.0375$ – 0.1 e/f.u.). When the cubic phase is dynamically stable ($n_{ph} > 0.1$ e/f.u.), we find accordingly that 000/000 is the lowest-energy structure, which is confirmed by the disappearance of polar atomic displacements and the cell shape distortions of all considered phases (see the Supplemental Material [31]). The predicted transition toward the 000/000 phase is consistent with the experimental observation, in BTO, of a downward shift of the Curie temperature under illumination [47]. Besides, the flattening of the energy landscape around 0.03 e/f.u. ($\approx 5 \times 10^{20}$ e.cm $^{-3}$) may be accompanied by a monoclinic phase transition (see the Supplemental Material [31]). We note that such a critical concentration would match recent observations of a monoclinic phase in BTO nanowires under illumination [12,48].

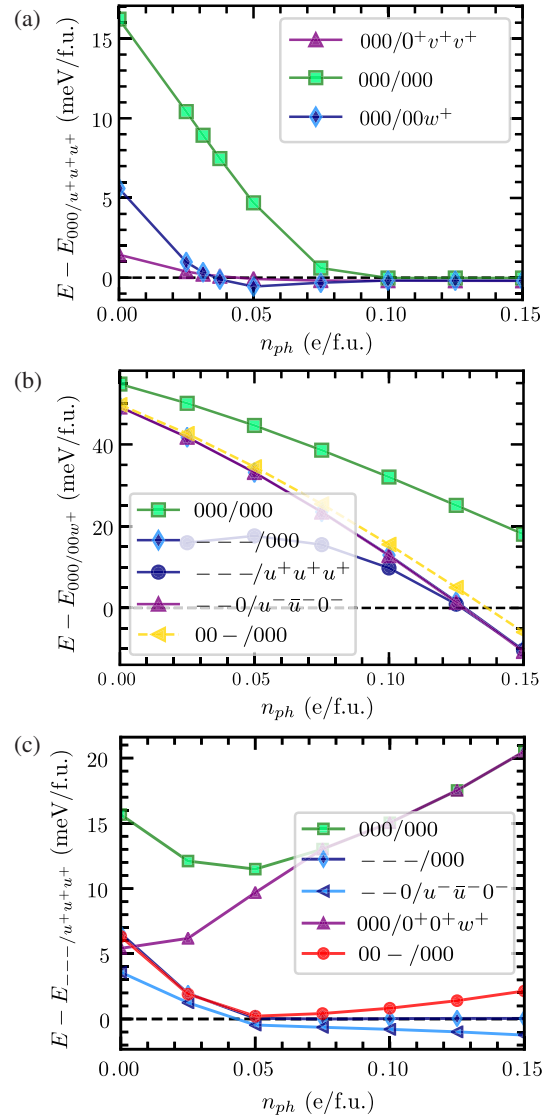


FIG. 3. (a) Energy of different phases in BTO with respect to the 000/ $u^+u^+u^+$ structure (dashed dark line), which is the ground state in the dark. The tetragonal 000/00 w^+ and then the cubic 000 phase become more energetically favorable. (b) Energy of different phases in PTO with respect to the 000/00 w^+ structure (dashed dark line), which is the ground state in the dark, showing that nonpolar antiferrodistortive phases become more stable at large concentration of photo-excited carriers. (c) Energy of different phases in PSTO with respect to the rhombohedral - - -/ $u^+u^+u^+$ structure (dashed dark line), which is the lowest energy phase considered when no carriers are excited.

PTO exhibits a single transition from the nonpolar cubic 000/000 phase to the ferroelectric tetragonal 000/00 w^+ structure below 765 K [15]. The phonon dispersion of the cubic phase for $n_{ph} = 0$ e/f.u. [Fig. 2(e)] exhibits one main polar instability at Γ , but also unstable modes at the R and M points associated with octahedra tilting 00- and 00+, respectively. The strength of the polar instability at Γ

decreases with increasing the number of photo-excited carriers [see Figs. 2(e) and 2(h)] as in BTO. However, it never totally disappears, indicating that ferroelectricity in PTO is more robust against photocarrier generation. In contrast, the strengths of the tilting instabilities at R and M are slightly enhanced, and they become dominant for $n_{\text{ph}} \geq 0.1$ [Figs. 2(g) and 2(h)], suggesting a transition from a polar to a nonpolar structure with oxygen tilts under illumination.

Hence, we compute the energies of several prototypical phases upon illumination, as shown in Fig. 3(b). The ferroelectric $000/00w^+$ phase, which is the ground state in dark conditions, is the black dashed baseline, while the cubic phase is plotted as green squares. We also plot a rhombohedral polar $---/u^+u^+u^+$ structure (navy circles) and its nonpolar counterpart, $a---/000$ (navy diamonds). We consider as well an orthorhombic phase (violet triangles) with the $---0/u^-\bar{u}^-0^-$ antipolar displacement pattern [49]. A $00c^-/000$ nonpolar tetragonal phase is also calculated (gold triangles). According to Fig. 3(b), the ferroelectric $000/00w^+$ phase is the most stable up to $n_{\text{ph}} \approx 0.125$ $e/f.u.$, the nonpolar phase with tilts becoming dominant beyond that point. Overall, the antipolar $---0/u^-\bar{u}^-0^-$ phase is slightly more favorable (by 0.2–0.3 meV/f.u.) than the $---/000$ phase for $n_{\text{ph}} \geq 0.125$ $e/f.u.$ Because of this small energy difference, it is impossible to predict with certainty the symmetry of PTO at large concentrations of photo-excited carriers, and we can only reckon that this should be a phase with oxygen tilts.

Unlike BTO, the polar atomic distortion in the $000/00w^+$ phase remains rather large under photo-excitation (see the Supplemental Material [31]). Moreover, both the antipolar displacement (for the $---0/u^-\bar{u}^-0^-$ phase) and the tilt angle (for $---/000$ and $---0/u^-\bar{u}^-0^-$) increase with n_{ph} . In contrast, the polar displacements of the $---/u^+u^+u^+$ phase disappear with increasing n_{ph} , and it thus collapses into the $---/000$ phase, confirming that tilts and polarization are competing order parameters in PTO [50,51], illumination tipping the balance toward the former.

Furthermore, calculations of minimum energy transition paths between phases (see the Supplemental Material [31]) show that $---0/u^-\bar{u}^-0^-$ and $---/000$ are unstable in the dark; however, the $000/00w^+$ phase remains metastable under illumination, drawing the picture of a first-order light-induced transition in PTO.

The large concentration of 0.125 $e/f.u.$ needed to destabilize the $000/00w^+$ phase in PTO is potentially outside the reach of experiments and certainly not desirable for applications. We can try to improve this situation by mixing PTO with an antiferrodistortive material such as SrTiO_3 and form the solid solution $(\text{Pb}_{1/2}\text{Sr}_{1/2})\text{TiO}_3$ (PSTO) to favor the tilt instability with respect to the polar one. As a proof of concept, several phases of PSTO with rocksalt order were calculated in Fig. 3(c). In particular, a

polar rhombohedral $---/u^+u^+u^+$ phase (black dashed line) is the ground state in the dark. The $000/00w^+$ (purple triangles) and the high-symmetry cubic $000/000$ phase (in green squares) have increasing energy with n_{ph} . On the contrary, the antipolar tilted phase $---0/u^-\bar{u}^-0^-$ (light blue triangles) becomes the most stable phase above $n_{\text{ph}} = 0.05$ $e/f.u.$, thus supporting the proposed design strategy to reduce the critical concentration for the polar-to-antipolar/antiferrodistortive transition.

From this work, it also becomes apparent that the ferroelectric instability can be hampered by the photo-generation of free carriers. Obviously, free carriers screen the long-range Coulombic interaction responsible for the polar order [32,52], thus seemingly disfavoring polar phases with respect to nonpolar ones. This is consistent with calculations [32,52] and experiments [53] performed by doping BTO with free electrons. The former predicted the disappearance of the polar order in BTO at a concentration of extra electrons of ≈ 0.1 $e/f.u.$, which is exactly the concentration of photo-excited carriers that stabilizes the cubic phase in our calculations. We also note that the destruction of the polar order in BTO and the large stability (and metastability) window of the $000/00w^+$ phase in PTO are consistent with the doping calculations performed in Ref. [32]. In addition, photoexcitation tends to move electrons from O $2p$ states to Ti d states, thus destroying the covalent bonding that drives the ferroelectric order [54] and favoring nonpolar orders. Looking at the evolution of interatomic force constants (IFCs) (see the Supplemental Material [31]) under photoexcitation shows that (i) almost all IFCs are reduced in magnitude under photoexcitation, and (ii) the most affected IFCs correspond to fourth nearest neighbors interaction, i.e., similar atoms (Ti-Ti, O-O, etc.) interacting along the $\langle 100 \rangle$ cubic directions. This parallels the further stabilization of the paraelectric phase under photoexcitation in the incipient ferroelectric PbTe, which results from screening of the long-range Coulomb interactions by the redistributed photoexcited carriers along the $\langle 100 \rangle$ cubic directions [55]. From the evidence presented here, as well as in other works involving doping and photoexcited calculations [32,55], electrostatic screening by photoexcited carriers appears as a universal mechanism for “dipole-dipole driven” ferroelectric materials such as BTO [33].

In addition, the volume of most phases decreases with increasing concentration of excited carriers in both BTO and PTO, except that of the cubic $000/000$ phase, which increases instead (see the Supplemental Material [31]). Interestingly, the decrease of volume of the polar phases is consistent with the disappearance of the polar order and is reminiscent of the well-known [17–19] effect of hydrostatic compression; yet, the volume increase of the cubic phase under illumination should in principle favor the polar instabilities. Hence, our results suggest that the behavior of the polar distortion upon illumination cannot be

understood solely in terms of a photoinduced volume change [34], and that screening effects play a central role.

There are, however, potential limitations of this work, since DFT is known to underestimate the quasi-particle bandgap. Furthermore, excitonic effects are described within a mean-field approximation using constrained DFT to mimic excited states occupations. First, we performed G_0W_0 [56] calculations with the YAMBO [35] package—using DFT input from QUANTUM ESPRESSO [36,37]—in order to accurately describe the conduction and valence bands (see the Supplemental Material [31]). The corrected band structure is overall not altered, except for an almost rigid upshift of the conduction bands. This shift slightly depends on the studied phase (with differences smaller than 100 meV between phases). The shift is smaller for nonpolar phases, therefore facilitating further the light-induced transitions toward such latter states.

For BTO, we checked the robustness of our conclusions by performing calculations of zone center phonons of the cubic phase with hybrid DFT. We compare calculations performed with the semilocal PBEsol functional and the hybrid HSEsol [38] functional. Both functionals give similar lattice constants and similar value for the imaginary frequency of the soft ferroelectric mode, even though the band gaps are quite different (1.8 eV for PBEsol and 3.4 eV, close to the GW value, for HSEsol). Despite the very different band gaps, the phonon frequencies as a function of the excited charge density evolve similarly: we observe a stabilization of the soft mode at an excited charge density of 0.09 electron per formula unit (see the Supplemental Material [31]). Hence, although our DFT-based description may slightly alter the critical concentrations at which transitions occur, the present qualitative behavior should be correct, especially given our results in Fig. 2 for the dynamical lattice instabilities of the *paraelectric cubic state*.

At last, let us discuss the possibility of having photoinduced phase transitions to (small self-trapped, or ST) polaronic states. Recent (doping) calculations have shown that ST holes were unlikely in PTO [57,58], but could potentially be stabilized in cubic BTO [57]. In order to check the appearance of polaronic states, we ran calculations in BaTiO₃ under photoexcitation with $n_{\text{ph}} = 0.075$ e/f.u. and $n_{\text{ph}} = 0.150$ e/f.u. (with no symmetry). No trace of polaronic states was found.

In conclusion, we have shown that light absorption is a viable route to switch on or off specific lattice instabilities in complex materials such as ferroelectric perovskite oxides. Via first-principles calculations we have demonstrated the microscopic mechanism leading to a light-controlled stabilization of the cubic phase in BTO but not in PTO. The calculations are a promising tool to engineer and optimize such light-triggered transformations, suggesting strategies for their practical realization in suitably chosen materials. The results presented in this work could offer a route to design light-controlled memory,

by accessing light-induced metastable states (see Fig. 4 in the Supplemental Material [31] and related discussion).

C. P. and L. B. thank the ARO Grant No. W911NF-16-1-0227. We also acknowledge support from the National Research Fund, Luxembourg through Project No. INTER/ANR/13/20/NANOTMD (E. T. and L. W.); Project No. INTER/ANR/16/11562984/EXPAND (J. I.) and the inter-mobility program (Grant No. 15/9890527/GREENOX, J. I. and L. B.). C. P. thanks the AHPCC and a DoD challenge grant for use of computing resources. We thank B. Dkhil and P. Ruello for interesting discussions.

*charles.paillard@centralesupelec.fr

†laurent@uark.edu

- [1] I. Grinberg, D. V. West, M. Torres, G. Gou, D. M. Stein, L. Wu, G. Chen, E. M. Gallo, A. R. Akbashev, P. K. Davies, J. E. Spannier, and A. M. Rappe, *Nature (London)* **503**, 509 (2013).
- [2] B. I. Sturman and V. M. Fridkin, *The Photovoltaic and Photorefractive Effects in Noncentrosymmetric Materials* (Gordon and Breach Science Publishers, Philadelphia, 1992).
- [3] L. Z. Tan, F. Zheng, S. M. Young, F. M. Wang, S. Liu, and A. M. Rappe, *npj Comput. Mater.* **2**, 16026 (2016).
- [4] C. Paillard, X. Bai, I. C. Infante, M. Guennou, G. Geneste, M. Alexe, J. Kreisel, and B. Dkhil, *Adv. Mater.* **28**, 5153 (2016).
- [5] R. Nechache, C. Harnagea, S. Li, L. Cardenas, J. Chakrabarty, and F. Rosei, *Nat. Photonics* **9**, 61 (2015).
- [6] B. Kundys, M. Viret, D. Colson, and D. O. Kundys, *Nat. Mater.* **9**, 803 (2010).
- [7] M. Lejman, G. Vaudel, I. C. Infante, P. Gemeiner, V. E. Gusev, B. Dkhil, and P. Ruello, *Nat. Commun.* **5**, 4301 (2014).
- [8] B. Kundys, *Appl. Phys. Rev.* **2**, 011301 (2015).
- [9] Y. Cui, J. Briscoe, and S. Dunn, *Chem. Mater.* **25**, 4215 (2013).
- [10] V. Iurchuk, D. Schick, J. Bran, D. Colson, A. Forget, D. Halley, A. Koc, M. Reinhardt, C. Kwamen, N. A. Morley, M. Bargheer, M. Viret, R. Gumenuik, G. Schmerber, B. Doudin, and B. Kundys, *Phys. Rev. Lett.* **117**, 107403 (2016).
- [11] R. Guo, L. You, Y. Zhou, Z. S. Lim, X. Zou, L. Chen, R. Ramesh, and J. Wang, *Nat. Commun.* **4**, 1990 (2013).
- [12] Y.-H. Kuo, S. Nah, K. He, T. Hu, and A. M. Lindenberg, *J. Mater. Chem. C* **5**, 1522 (2017).
- [13] A. M. Glazer, *Acta Crystallogr. Sect. B* **28**, 3384 (1972).
- [14] G. H. Kwei, A. C. Lawson, S. J. L. Billinge, and S. W. Cheong, *J. Phys. Chem.* **97**, 2368 (1993).
- [15] G. Shirane and S. Hoshino, *J. Phys. Soc. Jpn.* **6**, 265 (1951).
- [16] P. Ghosez, E. Cockayne, U. V. Waghmare, and K. M. Rabe, *Phys. Rev. B* **60**, 836 (1999).
- [17] I. A. Kornev, L. Bellaiche, P. Bouvier, P.-E. Janolin, B. Dkhil, and J. Kreisel, *Phys. Rev. Lett.* **95**, 196804 (2005).
- [18] P.-E. Janolin, P. Bouvier, J. Kreisel, P. A. Thomas, I. A. Kornev, L. Bellaiche, W. Crichton, M. Hanfland, and B. Dkhil, *Phys. Rev. Lett.* **101**, 237601 (2008).

- [19] M. Ahart, M. Somayazulu, R. E. Cohen, P. Ganesh, P. Dera, H.-k. Mao, R. J. Hemley, Y. Ren, P. Liermann, and Z. Wu, *Nature (London)* **451**, 545 (2008).
- [20] H. Moriwake, A. Konishi, T. Ogawa, C. A. J. Fisher, A. Kuwabara, and D. Fu, *J. Appl. Phys.* **119**, 064102 (2016).
- [21] A. Kirilyuk, A. V. Kimel, and T. Rasing, *Rev. Mod. Phys.* **82**, 2731 (2010).
- [22] A. Subedi, *Phys. Rev. B* **92**, 214303 (2015).
- [23] X. Gonze *et al.*, *Comput. Phys. Commun.* **180**, 2582 (2009).
- [24] P. E. Blöchl, *Phys. Rev. B* **50**, 17953 (1994).
- [25] M. Torrent, F. Jollet, F. Bottin, G. Zérah, and X. Gonze, *Comput. Mater. Sci.* **42**, 337 (2008).
- [26] J. P. Perdew, A. Ruzsinszky, G. I. Csonka, O. A. Vydrov, G. E. Scuseria, L. A. Constantin, X. Zhou, and K. Burke, *Phys. Rev. Lett.* **100**, 136406 (2008).
- [27] W. Kohn and L. J. Sham, *Phys. Rev.* **140**, A1133 (1965).
- [28] J. P. Perdew and Y. Wang, *Phys. Rev. B* **45**, 13244 (1992).
- [29] P. Würfel and U. Würfel, *Physics of Solar Cells: From Basic Principles to Advanced Concepts* (Wiley-VCH, Weinheim, 2009).
- [30] A. Togo and I. Tanaka, *Scr. Mater.* **108**, 1 (2015).
- [31] See Supplemental Material at <http://link.aps.org/supplemental/10.1103/PhysRevLett.123.087601> for more details which includes Refs. [12,14,17–19,32–46]. We detail the symmetry and atomic displacement evolution under excitation of carriers; nudge elastic band calculations show that the transition is likely to be first order and that the nonpolar phase are not metastable, but rather unstable; we discuss the occurrence of a monoclinic phase in BaTiO₃; volume changes under illumination are compared with hydrostatic pressure results from the literature. The evolution of interatomic force constants is also depicted. Finally, via the GW-approximation and hybrid DFT calculations, we discuss the relevance of many-body effects for the photo-induced stabilization of the cubic phase.
- [32] H. J. Zhao, A. Filippetti, C. Escorihuela-Sayalero, P. Delugas, E. Canadell, L. Bellaïche, V. Fiorentini, and J. Íñiguez, *Phys. Rev. B* **97**, 054107 (2018).
- [33] A. Filippetti, V. Fiorentini, F. Ricci, P. Delugas, and J. Íñiguez, *Nat. Commun.* **7**, 11211 (2016).
- [34] C. Paillard, S. Prosandeev, and L. Bellaïche, *Phys. Rev. B* **96**, 045205 (2017).
- [35] A. Marini, C. Hogan, M. Grüning, and D. Varsano, *Comput. Phys. Commun.* **180**, 1392 (2009).
- [36] P. Giannozzi *et al.*, *J. Phys. Condens. Matter* **21**, 395502 (2009).
- [37] P. Giannozzi *et al.*, *J. Phys. Condens. Matter* **29**, 465901 (2017).
- [38] L. Schimka, J. Harl, and G. Kresse, *J. Chem. Phys.* **134**, 024116 (2011).
- [39] H. D. Megaw, *Acta Crystallogr.* **5**, 739 (1952).
- [40] E. Weinan, W. Ren, and E. Vanden-Eijnden, *J. Chem. Phys.* **126**, 164103 (2007).
- [41] Z.-G. Ye, B. Noheda, M. Dong, D. E. Cox, and G. Shirane, *Phys. Rev. B* **64**, 184114 (2001).
- [42] L. Bellaïche, A. García, and D. Vanderbilt, *Phys. Rev. Lett.* **84**, 5427 (2000).
- [43] D. Sangalli, A. Ferretti, H. Miranda, C. Attaccalite, I. Marri, E. Cannuccia, P. Melo, M. Marsili, F. Paleari, A. Marrazzo, G. Prandini, P. Bonfà, M. O. Atambo, F. Affinito, M. Palummo, A. Molina-Sánchez, C. Hogan, M. Grüning, D. Varsano, and A. Marini, [arXiv:1902.03837](https://arxiv.org/abs/1902.03837).
- [44] C. Thomsen, H. T. Grahn, H. J. Maris, and J. Tauc, *Phys. Rev. B* **34**, 4129 (1986).
- [45] R. Dovesi, A. Erba, R. Orlando, C. M. Zicovich-Wilson, B. Civalleri, L. Maschio, M. Rerat, S. Casassa, J. Baima, S. Salustro, and B. Kirtman, *WIREs Comput. Mol. Sci.* **8**, e1354 (2018).
- [46] G. Sophia, P. Baranek, C. Sarrazin, M. Rerat, and R. Dovesi, *Phase Trans. Multinatl. J.* **86**, 1069 (2013).
- [47] L. Belyaev, V. M. Fridkin, A. A. Grekov, N. A. Kosonogov, and A. I. Rodin, *J. Phys. (Paris), Colloq.* **33**, C2 (1972).
- [48] Pump-probe experiments on BiFeO₃ in Ref. [7] estimate $n_{\text{ph}} \sim 5 \times 10^{19} e \text{ cm}^{-3}$ with maximum used fluences of $\sim 50 \mu\text{J cm}^{-2}$. In Ref. [12] (which observes a monoclinic phase in BaTiO₃ nanowires), fluences ranging up to $600 \mu\text{J cm}^{-2}$ are used, which would correspond to a carrier concentration of $\sim \frac{600}{50} \cdot 5 \times 10^{19} \approx 6 \times 10^{20} e \text{ cm}^{-3}$. This order of magnitude matches the region where we observed flattening of the energy landscape in Fig. 3(a) (around the $000/u^+u^+u^+$ to $000/00w^+$ transition) which could potentially harbor a monoclinic phase as discussed in the Supplemental Material Ref. [31].
- [49] L. Bellaïche and J. Íñiguez, *Phys. Rev. B* **88**, 014104 (2013).
- [50] I. A. Kornev, L. Bellaïche, P.-E. Janolin, B. Dkhil, and E. Suard, *Phys. Rev. Lett.* **97**, 157601 (2006).
- [51] J. C. Wojdeł, P. Hermet, M. P. Ljungberg, P. Ghosez, and J. Íñiguez, *J. Phys. Condens. Matter* **25**, 305401 (2013).
- [52] Y. Wang, X. Liu, J. D. Burton, S. S. Jaswal, and E. Y. Tsymlal, *Phys. Rev. Lett.* **109**, 247601 (2012).
- [53] J. Fujioka *et al.*, *Sci. Rep.* **5**, 13207 (2015).
- [54] R. E. Cohen, *Nature (London)* **358**, 136 (1992).
- [55] M. P. Jiang, M. Trigo, I. Savić, É. D. Murray, C. Bray, J. Clark, T. Henighan, M. Kozina, M. Chollet, J. M. Glowina, M. C. Hoffmann, D. Zhu, O. Delaire, A. F. May, B. C. Sales, A. M. Lindenberg, P. Zalden, T. Sato, R. Merlin, and D. A. Reis, *Nat. Commun.* **7**, 12291 (2016).
- [56] M. S. Hybertsen and S. G. Louie, *Phys. Rev. B* **34**, 5390 (1986).
- [57] P. Erhart, A. Klein, D. Åberg, and B. Sadigh, *Phys. Rev. B* **90**, 035204 (2014).
- [58] C. Paillard, G. Geneste, L. Bellaïche, and B. Dkhil, *J. Phys. Condens. Matter* **29**, 485707 (2017).